Available online at www.sciencedirect.com
ScienceDirect
Journal of Sound and Vibration 299 (2007) 164–177
JOURNAL OF SOUND AND VIBRATION
www.elsevier.com/locate/jsvi

Low-gravity liquid nonlinear sloshing analysis in a tank under pitching excitation

He Yuanjun[a,*], Ma Xingrui[b], Wang Pingping[a], Wang Benli[a]

[a]*Research Center of Satellite Technology, Harbin Institute of Technology, Harbin, Heilongjiang 150001, PR China*
[b]*China Aerospace Science and Technology Corporation, Beijing 100830, PR China*

Received 25 April 2006; received in revised form 3 July 2006; accepted 9 July 2006
Available online 15 September 2006

Abstract

Under pitch excitation, the sloshing of liquid in circular cylindrical tank includes planar motion, rotary motion and rotary motion inside planar motion. The boundaries between stable motion and unstable motion depend on the radius of the tank, the liquid height, the gravitational intension, the surface tensor and the sloshing damping. In this article, the differential equations of nonlinear sloshing are built first. And by variational principle, the Lagrange function of liquid pressure is constructed in volume integration form. Then the velocity potential function is expanded in series by wave height function at the free surface. The nonlinear equations with kinematics and dynamics free surface boundary conditions through variation are derived. At last, these equations are solved by multiple-scales method. The influence of Bond number on the global stable response of nonlinear liquid sloshing in circular cylinder tank is analyzed in detail. The result indicates that the system's amplitude–frequency response changes from a 'soft-spring' to a 'hard-spring' in the planar motion with the decreasing of the Bond number, while it changes from a 'hard-spring' to a 'soft-spring' in the rotary motion. At the same time, jump, lag and other nonlinear phenomena of liquid sloshing are discovered.

1. Introduction

The problem of liquid sloshing in moving or stationary containers remains of great concern to aerospace, civil, and nuclear engineers, physicists, designers of road tankers and ship tankers, and mathematicians [1]. Depending on the type of disturbance, container shape, sloshing damp, baffle and setting position, the free liquid surface can experience different types of motion including simple planar, nonplanar, rotational, irregular beating, symmetric, asymmetric, quasi-periodic and chaotic. Up to now, it has received considerable attention over the past few years by numerical methods, such as MAC method, VOF method, BRM, FEM and BEM, and analytical methods. Although numerical methods, which can avoid deficiency caused by the experiment, such as lack of time, external applied loads, initial conditions and measuring conditions, are widely used in study of the nonlinear sloshing of liquid, analytical methods are equivalently important to discover and explain all kinds of nonlinear phenomena of liquid sloshing. And the key point of studying

*Corresponding author. Tel.: +86 451 86402357 8508.
E-mail address: hithyj@163.com (H. Yuanjun).

0022-460X/$ - see front matter © 2006 Elsevier Ltd. All rights reserved.
doi:10.1016/j.jsv.2006.07.003

sloshing of liquid through analytical method is the treatment of the nonlinear terms of the discrete differential or variational equations, in order to describe violent sloshing [2].

Many studies are done on nonlinear sloshing in a circle cylindrical tank under normal gravity. Hutton [3] took the lead in using perturbation method to study liquid sloshing under lateral excitation, and the results were verified by experiment. Gou et al. [4] discovered the phenomena of synchronous Hopf bifurcation by the Galerkin method. Komatsu [5] used multiscale method to study nonlinear sloshing in tank with arbitrary geometries under lateral excitation. The results coincide well with the experiment results. Yin et al. [6] generalized this method to study nonlinearity under pitching. Under low gravity field, the surface tension is dominant and the liquid may be oriented randomly within the tank depending essentially upon the wetting characteristics of the tank wall. Due to the complexity of study and the validity of method, the study on nonlinear sloshing develops slowly. Experiment is widely used to obtain the parameters of sloshing, and then the parameters are used in the design of control system. Satterlee and Reynolds (1964), Dodge and Garza (1967), Bauer and Siekmann (1971), Peterson et al. (1989), Bauer and Siekmann (1971), Peterson et al. (1989) studied linear and nonlinear sloshing by analytical method in the circle cylindrical tank, a Yeh (1967), Concus et al. (1969), Chu (1970), Dodge and Garza (1970), Dodge et al. (1991), Hung and Lee (1992), Utsumi (1998, 2000) studied sloshing in an axisymmetrical container [7]. Utsumi also studied the sloshing in teardrop tanks [8]. The shape of liquid quiet surface, natural frequency and sloshing modal, forced response, sloshing damp, influence of liquid to tank wall, establishment of equivalent models, extraction of sloshing parameter and large amplitude nonlinear sloshing within the context of low gravity are all studied by former researchers [9]. Peterson et al. [10] studied nonlinear sloshing and nonlinear fluid sloshing coupled to the dynamics of a spacecraft. Van Schoor and Crawley [11] studied it by experiment, and the results were tested on Middeck's. In addition, Waterhouse [12] also particularly discussed the problem that soft-spring and hard-spring varying with the depth of liquid.

In this paper, volume integration of pressure formed Lagrange function of liquid sloshing in low gravity is built based on variational principle and the velocity potential function is expanded in series by wave height function at the free surface. Then the boundary conditions of kinematics and dynamics at the free surface is obtained. Finally, through analytical study by multiple scales method, variation of amplitude frequency response characteristics of the system with Bond, jump, lag and other nonlinear phenomena of liquid sloshing are investigated.

2. A variational principle for liquid sloshing under low gravity

2.1. Governing equations

In the present context, the container is forced to pitch and(or) yaw with an angular velocity vector $\Omega(t)$. Fig. 1 shows a 3-D cylindrical tank in motion. A Cartesian coordinate system O–XYZ is an inertial system, Z-axis is directed upward. A coordinate system o–xyz is fixed to the container in such a manner that x-axis is parallel to the undisturbed free surface and the z-axis is in coincidence with the center line of the tank. Here, $f(r)+e-C_0$ is the free surface of the liquid, where $f(r)$ is the quiet free surface, e is the distance between the undisturbed free surface and the x-axis, which is taken positive when the free surface is above the x-axis. C_0 is the distance from the lowest point at the free surface under low gravity to the free surface under normal gravity. h is the depth of liquid. The origin o is taken as the center of rotation. $\alpha_x(t)$ and $\alpha_y(t)$ is the angular of inclination of container at the time t.

It is assumed that the liquid is inviscid and incompressible, and the flow is irrotational. The liquid sloshing low gravity undergoing pitching and(or) yaw motion can be reduced to the following nonlinear, initial boundary value problem:

$$\nabla^2\Phi = 0 \quad \text{in } V, \tag{1}$$

$$\nabla\Phi\cdot\vec{n} = (\vec{\Omega}\times\vec{r})\cdot\vec{n} \quad \text{on } S_w, \tag{2}$$

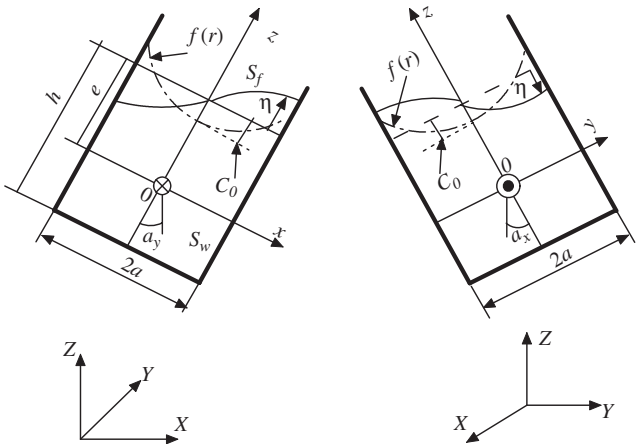

Fig. 1. A container under pitching and yawing excitation.

$$\frac{\partial \eta}{\partial t} = (\nabla \Phi - \vec{\Omega} \times \vec{r}) \cdot \nabla F \quad \text{on } S_f, \tag{3}$$

$$\frac{2H}{B_0} - \frac{\partial \Phi}{\partial t} - \frac{1}{2}|\nabla \Phi|^2 - \vec{r} + (\vec{\Omega} \times \vec{r}) \cdot \nabla \Phi = 0 \quad \text{on } S_f, \tag{4}$$

$$\frac{\partial \eta}{\partial r} = C_1 \operatorname{sgn}\left(\frac{\partial \eta}{\partial t}\right) \quad \text{at } r = a,\ z = f(a), \tag{5}$$

where V is the liquid region, $F = z - (\eta + e - C_0)$ is the equation of the free surface, η is the height of the free surface measured from the undisturbed free surface, $\vec{r}$ is the position vector of the liquid particle, $\vec{n}$ is the unit normal drawn outwardly on the wetted wall S_w, C_1 is constant of contact angle hysteresis, B_0 is Bond number. $2H$ is the mean surface curvature:

$$2H = \frac{1}{r}\frac{\partial}{\partial r}\left\{\frac{r\eta_r}{(1 + (f_r)^2)^{3/2}}\right\} + \frac{1}{r^2}\frac{\partial}{\partial \theta}\left\{\frac{\eta_\theta}{(1 + (f_r)^2)^{1/2}}\right\}. \tag{6}$$

2.2. A variational principle

By generalizing Luke's [13] stationary pressure principles, which are also applicable in the case of liquid forced responses, the Lagrange functions can be expressed in the form of volume integral of the liquid pressure. Then, by using the variational principles we can get

$$\delta J = \delta \int_{t_1}^{t_2} L(\Phi, \eta)\, \mathrm{d}t, \tag{7}$$

where

$$L(\Phi, \eta) = -\iint_V \int \left\{\frac{\partial \Phi}{\partial t} + \frac{1}{2}(\nabla \Phi)^2 - \frac{2H}{B_0} + \vec{r} - (\vec{\Omega} \times \vec{r}) \cdot \nabla \Phi\right\} \mathrm{d}V, \tag{8}$$

where $\Phi(r, \theta, z, t)$ and $\eta(r, \theta, t)$ are allowed to vary with time, but are subject to the restriction $\delta\Phi = 0$, $\delta\eta = 0$ at t_1 and t_2.

According to the usual procedure in the calculus of variations, Eq. (7) becomes

$$\delta J = -\int_{t_1}^{t_2}\left\{\iint\left[\left[\frac{\partial\Phi}{\partial t}+\frac{1}{2}(\nabla\Phi-\vec{\Omega}\times\vec{r})^2-\frac{1}{2}(\vec{\Omega}\times\vec{r})^2-\vec{r}\mp\frac{2\sigma H}{\rho}\right]\delta\eta\right]_{z=\eta+e}\mathrm{d}S_0 + \iint\left[\int_{-(h-e)}^{(\eta+e)}[\delta\Phi_t+(\nabla\Phi-\vec{\Omega}\times\vec{r})\cdot\nabla\delta\Phi]\,\mathrm{d}z\right]\mathrm{d}S_0\right\}\mathrm{d}t=0, \tag{9}$$

where S_0 is the cross-section of the container. Integrating the term $\delta\Phi_t$ in Eq. (9) with respect to z, and applying Green's first theorem, Eq. (7) can be rewritten as

$$\delta J = -\int_{t_1}^{t_2}\left\{\iint\left[\delta\eta\cdot\left[\frac{\partial\Phi}{\partial t}+\frac{1}{2}(\nabla\Phi-\vec{\Omega}\times\vec{r})^2-\frac{1}{2}(\vec{\Omega}\times\vec{r})^2-\vec{r}\mp\frac{2\sigma H}{\rho}\right]\right]_{z=\eta+e}\mathrm{d}S_0 - \iiint\delta\Phi\nabla^2\Phi\,\mathrm{d}V+\iint_{S_0}\left[\delta\Phi\cdot\left[-\frac{\partial\eta}{\partial t}+(\nabla\Phi-\vec{\Omega}\times\vec{r})\cdot\nabla F\right]\right]_{z=\eta+e}\mathrm{d}S_0 + \iint_{S_w}[\delta\Phi\cdot[\nabla\Phi\cdot\vec{n}-(\vec{\Omega}\times\vec{r})\cdot\vec{n}]]\,\mathrm{d}S\right\}\mathrm{d}t=0. \tag{10}$$

Considering that $\delta\eta$, $\delta\Phi$ may be given arbitrary independent values, we can also obtain Eqs. (1)–(4), but we should note that the variational principle does not include the contact line condition which requires that the contact angle between liquid surface and container wall remains constant during sloshing. Subsequently we will study the sloshing of liquid in a 3-D cylindrical, rigid open tank without baffles, which is forced to nonlinear harmonic pitching oscillation.

3. Nonlinear sloshing of liquid

The tank model and coordinate system are shown in Fig. 1. The tank is only forced to pitch around the y-axis with angular velocity Ω. The motion of the tank is given as

$$\alpha=\theta_0\sin\omega_e t, \tag{11}$$

where α is the angular of inclination of the tank, θ_0 is the peak amplitude of the tank pitching motion excitation and ω_e is an angular velocity.

Integrating $\partial\Phi_t/\partial t$ in Eq. (10) with respect to z, and expanding terms by the power series of η, and retaining the term up to the fourth order, Eq. (10) becomes

$$L=\iint_{S_0}\left[\left(\Phi+\widehat{\eta}\cdot\Phi_z+\Phi_{zz}\cdot\frac{\widehat{\eta}^2}{2}\right)\eta_t-\frac{1}{2}\Phi\cdot\Phi_z-\frac{(\nabla\Phi)^2}{2}\cdot\widehat{\eta} -\frac{\widehat{\eta}^2}{2}\left(\nabla\Phi\cdot\nabla\frac{\partial\Phi}{\partial z}\right)-\Phi r\Omega\cos\theta+\widehat{\eta}\cdot[(\vec{\Omega}\times\vec{r})\cdot\nabla\Phi] +\frac{\widehat{\eta}^2}{2}\left[\frac{\partial[(\vec{\Omega}\times\vec{r})\cdot\nabla\Phi]}{\partial z}\right]+r\sin a\cos\theta\,\widehat{\eta}-\cos a\cdot\frac{\widehat{\eta}^2}{2}-\cos a\cdot e\,\widehat{\eta} -\frac{1}{B_0}\cdot(2H)-\frac{1}{B_0}\frac{\partial(2H)}{\partial z}\widehat{\eta}\right]\mathrm{d}S-\frac{1}{2}\int[\Phi\Omega z\cos\theta]\,\mathrm{d}S|_{r=a} -\frac{1}{2}\int(\Phi\Omega r\cos\theta)\,\mathrm{d}S|_{z=e-h}, \tag{12}$$

where $\hat{\eta}=\eta+f(r)-C_0$. Thus it can be seen that the integrals over the free surface S_f have been transformed into those over the liquid quiet surface S_0.

The solution of Φ and η is searched by the summation form of the eigenmodes as follows

$$\Phi(r,\theta,z,t)=\Phi_0\Omega+\sum_n a_n\phi_n(r,\theta,z),\quad \eta(r,\theta,t)=\sum_n b_n\phi_n(r,\theta,0), \tag{13}$$

where $\Phi_0\Omega$ takes care of the inhomogeneous body boundary condition. We found Φ_0 when solving the linear equations (1)–(4) and it is

$$\Phi_0=a^2\left[\frac{z}{a}\cdot\frac{r}{a}-2\sum_{n=1}^{\infty}\left(\frac{ch[k_{1n}(z+h)]-2ch[k_{1n}z]}{\xi_{1n}(\xi_{1n}^2-1)sh(k_{1n}h)}\right)\cdot\frac{J_1(k_{1n}r)}{J_1(\xi_{1n})}\right]\cos\theta, \tag{14}$$

where J_n is the Bessel function of the first kind.

Substituting Eq. (13) into Eq. (12) and carrying out integrations, L can be expressed finally as

$$\begin{aligned}
L=\;&T^*/B_0+\sin a\cdot\tau+V^*/B-0.5\cos a\cdot W^*+\sum_i(\Omega\dot b_i\delta_i+a_i\beta_i\dot b_i-0.5\Omega\lambda_i a_i\delta_i\\
&-0.5\lambda_i a_i^2\beta_i-\Omega a_i\tau_i+\sin a\cdot b_i\tau_i-0.5\cos a\cdot b_i^2\beta_i+b_iT_i/B_0+0.5a_i\zeta_i\\
&+0.5a_i\varsigma_i+\Omega a_iW_i-\Omega a_iV_i-\Omega\lambda_i a_iU_i-\cos a\cdot b_iP_i+0.5\Omega a_iQ_i\\
&+0.5\Omega\lambda_i a_i\mathrm{I}Q_i-0.5\Omega a_iO_i-0.5\Omega\lambda_i a_i\mathrm{I}O_i-0.5\Omega k_i a_i\mathrm{I}P_i)\\
&+\sum_{i,j}((\lambda_iX_{ij}-0.5\Omega k_iY_{ij}^*)a_i\dot b_j+(\Omega E_{ij}^*-\Omega F_{ij}^*-\Omega\lambda_iE_{ij}^*-0.5P_{ij}-0.5O_{ij}\\
&-\Omega\mathrm{I}W_{ij}+\Omega\lambda_i\mathrm{I}V_{ij}-\Omega\lambda_i\mathrm{I}U_{ij}-\Omega\mathrm{I}P_{ij}-\Omega k_i\mathrm{I}O_{ij})a_ib_j-(0.5\lambda_i\mathrm{I}R_{ij}\\
&+0.5\lambda_i\lambda_jX_{ij}+0.5\lambda_i\mathrm{I}S_{ij}+0.5\lambda_ik_jY_{ij}^*)a_ia_j)+\sum_{i,j,k}((\lambda_i\alpha_{ij}^k+k_i\mathrm{I}T_{ijk})a_ib_j\dot b_k\\
&-0.5(\beta_{ij}^k+\gamma_{ij}^k+\lambda_iS_{ijk}+\lambda_i\lambda_j\alpha_{ij}^k+\lambda_ik_j\mathrm{I}T_{ijk})a_ia_jb_k+0.5\Omega(H_{ijk}^*+\lambda_iI_{ijk}^*\\
&-J_{ijk}^*-\lambda_iK_{ijk}^*-k_iL_{ijk}^*-\lambda_iR_{ijk})a_ib_jb_k+\sum_{i,j,k,l}(0.5k_ia_ib_jb_k\dot b_l\Gamma_{ij}^{kl}\\
&-0.5(\lambda_i\Lambda_{ij}^{kl}+\lambda_i\Delta_{ij}^{kl}+\lambda_ik_j\Gamma_{ij}^{kl})a_ia_jb_kb_l),
\end{aligned} \tag{15}$$

where dot denotes the derivatives with respect to time and T^*, W_i, X_{ij}, Y_{ij}^*, δ_i, β_i, α_{ij}^k, β_{ij}^k, Π_{ij}^{kl}, Γ_{ij}^{kl}, etc., can be got by calculating linear eigenvalues, which are given in the appendix.

Use the Lagrange function L, and variational functions, we can get the following set of two coupled equations

$$\beta_m(\lambda_ma_m-\dot b_m)=I\Re_m+\sum_i I\Re_i+\sum_{i,j}I\Re_{i,j}+\sum_{i,j,k}I\Re_{i,j,k}, \tag{16}$$

$$\beta_m(\dot a_m-b_m)=\mathrm{II}\Re_m+\sum_i\mathrm{II}\Re_i+\sum_{i,j}\mathrm{II}\Re_{i,j}+\sum_{i,j,k}\mathrm{II}\Re_{i,j,k}, \tag{17}$$

where $I\Re_m,\ldots,\mathrm{II}\Re_{i,j,k}$ are summations of corresponding terms (which is not given here). These equations show the free surface kinematic and the dynamic boundary condition.

4. Solve equations of the nonlinear sloshing

The method of multiple scales is used to solve Eqs. (16) and (17). Here independent variables T_n are introduced such as follows

$$T_n=\varepsilon^n t\quad\text{for } n=0,1,2,\ldots,$$

where ε is a measure of the amplitude of motion, which is small but finite. It is assumed that the solution of the coupled equations can be represented by expansions in such form

$$a_k(t)=\varepsilon a_{k1}(T_0,T_1,T_2\ldots)+\varepsilon^2a_{k2}(T_0,T_1,T_2\ldots)+\varepsilon^3a_{k3}(T_0,T_1,T_2\ldots)+\cdots, \tag{18}$$

$$b_k(t) = \varepsilon b_{k1}(T_0, T_1, T_2 \ldots) + \varepsilon^2 b_{k2}(T_0, T_1, T_2 \ldots) + \varepsilon^3 b_{k3}(T_0, T_1, T_2 \ldots) + \cdots. \tag{19}$$

Substituting Eqs. (18), (19) into Eqs. (16), (17) and equating the coefficients ε, ε^2,ε^3 to zero (detailed solution can be found by Eqs. (17)–(30) in paper [6]). First, the general solutions of the order ε, ε^2 can be written as

$$a_{m1}(T_0, T_1, T_2 \ldots) = A_m e^{i\omega_m T_0} + \text{cc}, \tag{20}$$

$$b_{m1}(T_0, T_1, T_2 \ldots) = -i\omega A_m e^{i\omega_m T_0} + \text{cc}, \tag{21}$$

$$\begin{aligned} a_{m2} = \sum_{i,j} [&E^m_{1,ij} A_i A_j e^{i(\omega_i+\omega_j)T_0} + E^m_{2,ij} A_i A_j e^{i(\omega_i-\omega_j)T_0} \\ &+ iE^m_{3,ij} A_i A_j e^{i(\omega_i+\omega_j)T_0} + iE^m_{4,ij} A_i A_j e^{i(\omega_i-\omega_j)T_0}] + \text{cc}, \end{aligned} \tag{22}$$

$$\begin{aligned} b_{m2} = \sum_{i,j} [&F^m_{1,ij} A_i A_j e^{i(\omega_i+\omega_j)T_0} + F^m_{2,ij} A_i A_j e^{i(\omega_i-\omega_j)T_0} \\ &+ iF^m_{3,ij} A_i A_j e^{i(\omega_i+\omega_j)T_0} + iF^m_{4,ij} A_i A_j e^{i(\omega_i-\omega_j)T_0}] + \text{cc}, \end{aligned} \tag{23}$$

where ω_m is the mth eigencircular frequency, A_m is the complex amplitude, cc stands for the complex conjugate of the preceding terms, i is the imaginary unit unless used as a suffix, $E^m_{1,ij}$, $E^m_{2,ij}$, $E^m_{3,ij}$, $E^m_{4,ij}$, $F^m_{1,ij}$, $F^m_{2,ij}$, $F^m_{3,ij}$, $F^m_{4,ij}$ are all real.

Finally, substituting a_{m1}, a_{m2}, b_{m1}, b_{m2} into equations of the ε^3, and eliminating the term b_{m3} yields

$$\begin{aligned} \beta_m(D_0^2 a_{m3} + \lambda_m a_{m3}) = &- D_0 Q_m - i2\omega_m D_2 A_m e^{i\omega_m T_0} \\ &+ \sum_{i,j,p,q} \vartheta_1(m;i,j;p,q) A_i A_p A_q e^{i(\omega_i+\omega_p+\omega_q)T_0} \\ &+ \sum_{i,j,s,t} \vartheta_5(m;i,j;s,t) A_j A_s A_t e^{i(\omega_j+\omega_s+\omega_t)T_0} \\ &+ \sum_{i,j,k} \hbar_1(m;i,j,k) A_i A_j A_k e^{i(\omega_i+\omega_j+\omega_k)T_0} \\ &+ \sum_{i,j,p,q} [\vartheta_2(m;i,j;p,q) \overline{A}_i A_p A_q e^{i(-\omega_i+\omega_p+\omega_q)T_0} \\ &+ \vartheta_3(m;i,j;p,q) A_i A_p \overline{A}_q e^{i(\omega_i+\omega_p-\omega_q)T_0} \\ &+ \vartheta_4(m;i,j;p,q) A_i \overline{A}_p A_q e^{i(\omega_i-\omega_p+\omega_q)T_0}] \\ &+ \sum_{i,j,s,t} [\vartheta_6(m;i,j;s,t) A_j \overline{A}_s A_t e^{i(\omega_j-\omega_s+\omega_t)T_0} \\ &+ \vartheta_7(m;i,j;s,t) \overline{A}_j A_s A_t e^{i(-\omega_j+\omega_s+\omega_t)T_0} \\ &+ \vartheta_8(m;i,j;s,t) A_j A_s \overline{A}_t e^{i(\omega_j+\omega_s-\omega_t)T_0}] \\ &+ i \sum_{i,j,p,q} \mathsf{F}_1(m;i,j;p,q) A_i A_p A_q e^{i(\omega_i+\omega_p+\omega_q)T_0} \\ &+ i \sum_{i,j,s,t} \mathsf{F}_5(m;i,j;s,t) A_j A_s A_t e^{i(\omega_j+\omega_s+\omega_t)T_0} \\ &+ i \sum_{i,j,p,q} [\mathsf{F}_2(m;i,j;p,q) \overline{A}_i A_p A_q e^{i(-\omega_i+\omega_p+\omega_q)T_0} \\ &+ \mathsf{F}_3(m;i,j;p,q) A_i A_p \overline{A}_q e^{i(\omega_i+\omega_p-\omega_q)T_0} \\ &+ \mathsf{F}_4(m;i,j;p,q) A_i \overline{A}_p A_q e^{i(\omega_i-\omega_p+\omega_q)T_0}] \end{aligned}$$

$$
\begin{aligned}
&+ i\sum_{i,j,s,t}[\mathsf{F}_6(m;i,j;s,t)A_j\overline{A}_sA_te^{i(\omega_j-\omega_s+\omega_t)T_0}\\
&+\mathsf{F}_7(m;i,j;s,t)\overline{A}_jA_sA_te^{i(-\omega_j+\omega_s+\omega_t)T_0}\\
&+\mathsf{F}_8(m;i,j;s,t)A_jA_s\overline{A}_te^{i(\omega_j+\omega_s-\omega_t)T_0}]\\
&+\sum_{i,j,k}[\hbar_2(m;i,j,k)\overline{A}_iA_jA_ke^{i(-\omega_i+\omega_j+\omega_k)T_0}\\
&+\hbar_3(m;i,j,k)A_iA_j\overline{A}_ke^{i(\omega_i+\omega_j-\omega_k)T_0}\\
&+\hbar_4(m;i,j,k)A_i\overline{A}_jA_ke^{i(\omega_i-\omega_j+\omega_k)T_0}]+\text{cc},
\end{aligned}
\tag{24}
$$

where $D_m=\partial/\partial T_m$. Each parameter is expressed as their respective coefficient in Eq. (24), we do not give them here. In the subsequent analysis when a circle cylindrical tanks undergo pitch excitation, the liquid surface will swell into a large amplitude breaking waves in the neighborhood of the resonant frequencies.

Here, taking the example of cylindrical tank under transverse excitation, whose frequency is close to the first-order inherent frequency of the liquid in the tank, nonlinear sloshing of liquid in cylindrical tank are discussed in three different conditions.

4.1. Planar motion

In the planar motion, ϕ and η can be expressed as

$$
\begin{aligned}
\phi_n(r,\theta,z)&=\frac{J_n(k_{nm}r)}{J_n(\xi_{nm})}\cdot\frac{\cosh[(k_{nm}(z+h))]}{k_{nm}\sinh[k_{nm}h]}\cos(n\theta),\\
\eta_n(r,\theta,0)&=\frac{J_n(k_{nm}r)}{J_n(\xi_{nm})}\cdot\frac{\cosh[(k_{nm}h)]}{k_{nm}\sinh[k_{nm}h]}\cos(n\theta),
\end{aligned}
$$

where $\xi_{nm}=k_{nm}a$, and wavenumber k_{nm} is the eigenvalue for mode (n,m), representing the solution of $J'_n(ka)=0$.

When the tank is subjected to the pitch excitation at the circular frequency Ω in the neighborhood of ω_m, A_m can be assumed as

$$
|A_m|\gg|A_i|\quad\text{for } i\neq m. \tag{25}
$$

Then Eq. (24) becomes

$$
\begin{aligned}
\beta_m(D_0^2a_{m3}+\lambda_ma_{m3})=&-D_0Q_m-i2\omega_m\beta_m\frac{\partial A_m}{\partial T_2}e^{i\omega_mT_0}+C_NA_m^2\overline{A}_me^{i\omega_mT_0}\\
&+C_TA_m^3e^{i3\omega_mT_0}+iD_NA_m^2\overline{A}_me^{i\omega_mT_0}+iD_TA_m^3e^{i3\omega_mT_0}+\text{cc},
\end{aligned}
\tag{26}
$$

where C_N, C_T, D_N and D_T are all real.

Since A_m is not a function of T_1, the difference between Ω and ω_m turns out to be of order ε^2 resulting in

$$
\Omega=\omega_m+\varepsilon^2\sigma. \tag{27}
$$

To obtain σ, Q_m and A_m are to be expressed as

$$
Q_m=\frac{1}{2}q_me^{i\Omega t}+\text{cc},\quad A_m=\frac{1}{2}\chi\cdot e^{\gamma}, \tag{28}
$$

where q_m, χ and γ are all real. When the small parameter ε takes the different measures, the useful range of detuning σ will change significantly. Substituting Eq. (28) into Eq. (26), equating the secular term to zeros, separating real part and imaginary part, the following equations are obtained as

$$
\begin{aligned}
\omega_m\beta_m\chi\frac{\partial\gamma}{\partial T_2}-\frac{1}{2}\Omega q_m\sin(\sigma T_2-\gamma)+\frac{1}{8}C_N\chi^3=0,\\
-\omega_m\beta_m\frac{\partial\chi}{\partial T_2}+\frac{1}{2}\Omega q_m\cos(\sigma T_2-\gamma)+\frac{1}{8}D_N\chi^3=0.
\end{aligned}
$$

Transformed them to autonomy system by $\vartheta = \sigma T_2 - \gamma$

$$\omega_m \beta_m \chi\left(\sigma - \frac{\partial \vartheta}{\partial T_2}\right) + \frac{1}{2}\Omega q_m \sin\vartheta + \frac{1}{8} C_N \chi^3 = 0,$$
$$-\omega_m \beta_m \frac{\partial \chi}{\partial T_2} + \frac{1}{2}\Omega q_m \cos\vartheta + \frac{1}{8} D_N \chi^3 = 0. \tag{29}$$

For the stable motion $\partial\chi/\partial T_2 = 0$, $\partial\vartheta/\partial T_2 = 0$. Equating the phase angle ϑ in Eq. (29), we can get the frequency-response equation as

$$\sigma = -\frac{C_N}{8\omega_m\beta_m}\chi^2 \pm \frac{\sqrt{16 q_m^2 \omega_m^2 - D_N^2 \chi^6}}{8\beta_m \omega_m \chi}. \tag{30}$$

Transforming Eq. (30), we can easily solve χ by Kardan theory.

And then the stability can be discussed by the behavior of small perturbations by letting

$$\chi = \chi_0 + \chi_p \quad (|\chi_p| \ll |\chi_0|), \tag{31}$$

$$\vartheta = \vartheta_0 + \vartheta_p \quad (|\vartheta_p| \ll |\vartheta_0|), \tag{32}$$

where (χ_0, ϑ_0) are the singular point solutions and (χ_p, ϑ_p) are small perturbations. Substituting Eqs. (31) and (32) into Eq. (29), and retaining the linear term, Eq. (29) becomes

$$\frac{\partial \chi_p}{\partial T_2} = \frac{3 D_N \chi_0^2}{8\omega_m\beta_m}\chi_p - \chi_0\left(\sigma + \frac{C_N}{8\omega_m\beta_m}\chi_0^2\right)\vartheta_p, \tag{33}$$

$$\frac{\partial \vartheta_p}{\partial T_2} = \frac{D_N \chi_0^2}{8\omega_m\beta_m}\vartheta_p + \frac{1}{\chi_0}\left(\sigma + \frac{3C_N}{8\omega_m\beta_m}\chi_0^2\right)\chi_p. \tag{34}$$

Then expressing the solution for these equations as

$$\chi_p = \chi_{p0} e^{\overline{\lambda} T_2}, \quad \vartheta_p = \vartheta_{p0} e^{\overline{\lambda} T_2}. \tag{35}$$

Substituting them into Eqs. (33) and (34) yields the characteristic equation for $\overline{\lambda}$ and obtaining $\overline{\lambda}$.

$$\overline{\lambda}^2 - \frac{D_N \chi_0^2}{2\omega_m\beta_m}\overline{\lambda} + \frac{3 D_N^2 \chi_0^4}{64\omega_m^2\beta_m^2} + \left(\sigma + \frac{3C_N}{8\omega_m\beta_m}\chi_0^2\right)\left(\sigma + \frac{C_N}{8\omega_m\beta_m}\chi_0^2\right) = 0,$$

$$\overline{\lambda}_{1,2} = \frac{D_N\chi_0^2}{4\omega_m\beta_m} \pm \frac{1}{2}\sqrt{\frac{D_N^2\chi_0^4}{16\omega_m^2\beta_m^2} - 4\left(\sigma + \frac{3C_N}{8\omega_m\beta_m}\chi_0^2\right)\left(\sigma + \frac{C_N}{8\omega_m\beta_m}\chi_0^2\right)}. \tag{36}$$

The stable–unstable regions are given in the (σ, χ) yield

$$\left(\sigma + \frac{3C_N}{8\omega_m\beta_m}\chi_0^2\right)\left(\sigma + \frac{C_N}{8\omega_m\beta_m}\chi_0^2\right) = \frac{D_N^2\chi_0^4}{64\omega_m^2\beta_m^2}. \tag{37}$$

We can get the response up to the second order as

$$\phi(r,\theta,z,t) = (\varepsilon\chi)\cos(\Omega t - \varphi)\psi_m(r,\theta,z) - \frac{1}{2}(\varepsilon\chi)^2 \sin 2(\Omega t - \varphi)\sum_i E^i_{1,mm}\psi_i(r,\theta,z), \tag{38}$$

$$\eta(r,\theta,t) = \omega_m(\varepsilon\chi)\sin(\Omega t - \varphi)\psi_m(r,\theta,0) + \frac{1}{2}(\varepsilon\chi)^2\sum_i [F^i_{1,mm}\cos(\Omega t - \varphi) + F^i_{2,mm}]\psi_i(r,\theta,0), \tag{39}$$

where $-\varphi$ is phase angle, which obtained by Eq. (29)

$$\varphi = \arctan\frac{C_N\chi^2 + 8\omega_m\beta_m\sigma}{D_N\chi^2}. \tag{40}$$

It is phase-frequency relation of stable response. Formula (38) indicates that constant part of velocity potential function is zero, and formula (39) indicates that there exists a constant part in the second order similar wave height function, namely the zero shift of the stable response of the nonlinear liquid sloshing.

4.2. Constant amplitude rotary motion

Based on the experimental and numerical results, even though the circle cylindrical tank just undergoes lateral excitation, when the frequency lays in appropriate range, rotary motion occurs. Here rotary motion can be categorized into three types. Firstly, there is evidently out of surface sloshing phenomenon in the transition process, which takes the form of rotating in random directions, either left or right. However, the phenomena will disappear eventually after stepping into the stable state. Secondly, the phenomenon will not disappear in the stable state, but presents a similar 'beat' phenomenon within and out of the surface. Thirdly, the surface rotates in the same direction all the time, that is to say both in the transition and stable states, either clockwise or anticlockwise but the amplitude of the sloshing within and out of the surface under a certain excitation is constant. And here we will concentrate on the analysis of the third condition. As a result of the existence of the 90° phase differences between the planar motion and rotary motion eigenmode, the rotary motion can be expressed as

$$\phi_n(r,\theta,z)=\frac{J_n(k_{nm}r)}{J_n(\xi_{nm})}\cdot\frac{\cosh[(k_{nm}(z+h))]}{k_{nm}\sinh[k_{nm}h]}\,(\cos(n\theta)+\mathrm{i}\,\sin(n\theta)).$$

Replacing the mode suffix m in Eq. (24) by 1_c and 1_s, and equating the secular terms to zero, the following equations are obtained as:

$$\begin{aligned}&-2\mathrm{i}\omega_1\beta_1\frac{\partial A_{1c}}{\partial T_2}\,\mathrm{e}^{\mathrm{i}\omega_1 T_0}+\frac{1}{2}q_{1c}\Omega\mathrm{e}^{\mathrm{i}\Omega t}+(C_N A_{1c}\overline{A}_{1c}A_{1c}+C_{s1}A_{1s}\overline{A}_{1s}A_{1c}\\&+C_{s2}A_{1s}A_{1s}\overline{A}_{1c})\mathrm{e}^{\mathrm{i}\omega_1 T_0}+\mathrm{i}(D_N A_{1c}\overline{A}_{1c}A_{1c}+D_{s1}A_{1s}\overline{A}_{1s}A_{1c}\\&+D_{s2}A_{1s}\overline{A}_{1c}A_{1s})\mathrm{e}^{\mathrm{i}\omega_1 T_0}+\mathrm{cc},\end{aligned}\tag{41}$$

$$\begin{aligned}&-2\mathrm{i}\omega_1\beta_1\frac{\partial A_{1s}}{\partial T_2}\,\mathrm{e}^{\mathrm{i}\omega_1 T_0}+(C_N A_{1s}\overline{A}_{1s}A_{1s}+C_{s1}A_{1c}\overline{A}_{1c}A_{1s}+C_{s2}A_{1c}A_{1c}\overline{A}_{1s})\mathrm{e}^{\mathrm{i}\omega_1 T_0}\\&+\mathrm{i}(D_N A_{1s}\overline{A}_{1s}A_{1s}+D_{s1}A_{1c}\overline{A}_{1c}A_{1s}+D_{s2}A_{1c}\overline{A}_{1s}A_{1c})\mathrm{e}^{\mathrm{i}\omega_1 T_0}+\mathrm{cc},\end{aligned}\tag{42}$$

where ω_1 and β_1 represent ω_{1c}, ω_{1s} and β_{1c}, β_{1s} respectively. C_{s1}, C_{s2}, D_{s1} and D_{s2} are all real.

These two equations (41) and (42) express the motions that have 90° phase difference. Theoretically, the four unknown variables can be determined by aggregating the above equations, but actually it is quite difficult in solving them. According to the experiment results and numerical analysis, despite in the constant amplitude rotary motion the sloshing amplitude within and out of the surface are not strictly equal, the difference is quite small. Here two assumptions are made for the convenience of further analytical procedures.

First, in the constant amplitude rotary motion the two amplitudes within and out of surface are strictly equivalent.

Secondly, in the constant amplitude rotary motion, there is a constant 90° phase difference between the sloshing motions within and out of surface.

The rotary motion is expressed as

$$A_{1c}=\frac{1}{2}\chi\mathrm{e}^{\mathrm{i}\varphi},\quad A_{1s}=-\frac{i}{2}\chi\mathrm{e}^{\mathrm{i}\varphi}.\tag{43}$$

Multiplying 'i' to each side of Eq. (42), adding it to Eq. (41), and then making similar processes to planar motion through Eq. (43), therefore the nonlinear frequency and phase-response equation becomes

$$\sigma=-\frac{C_N+C_{s1}-C_{s2}}{8\omega_m\beta_m}\,\chi^2\pm\frac{\sqrt{16q_m^2\omega_m^2-(D_N+D_{s1}-D_{s2})^2\chi^6}}{8\beta_m\omega_m\chi},\tag{44}$$

$$\gamma = \arctan \frac{(C_N + C_{s1} - C_{s2})\chi^2 + 8\omega_m\beta_m\sigma}{(D_N + D_{s1} - D_{s2})\chi^2}. \tag{45}$$

The stable–unstable regions are given in the (σ, χ) yield

$$\left(\sigma + \frac{3(C_N + C_{s1} - C_{s2})}{8\omega_m\beta_m}\chi_0^2\right)\left(\sigma + \frac{C_N + C_{s1} - C_{s2}}{8\omega_m\beta_m}\chi_0^2\right) = \frac{(D_N + D_{s1} - D_{s2})^2}{64\omega_m^2\beta_m^2}\chi_0^4. \tag{46}$$

Due to the difficulty to analyze the stable rotary motion with random directions, we will discuss the situation separately.

4.3. Appearance of rotary motion in planar motion

When the phenomenon jump or rotary motion appears, the planar motion will become unstable. Since the former phenomenon has been discussed before, we will concentrate on the latter one. Let

$$A_{1c} = \frac{1}{2}\chi_0 e^{i\varphi}, \quad A_{1s} = -\frac{i}{2}\chi_p e^{i\varphi}. \tag{47}$$

And then consider the condition of

$$|\chi_p| \ll |\chi_0|. \tag{48}$$

Then the following result can be derived from Eqs. (41), (42)

$$\begin{aligned} &-i\omega_1\left[\frac{\partial\chi_0}{\partial T_2} + \frac{\partial\chi_p}{\partial T_2} + i(\chi_0 + \chi_p)\left(\sigma - \frac{\partial\varphi}{\partial T_2}\right)\right] - \frac{1}{2}i\Omega q_1 e^{i\varphi} \\ &+ \frac{1}{8}\chi_0^2[C_N\chi_0 + (C_{s1} - C_{s2})\chi_p] - \frac{i}{8}\chi_0^2[D_N\chi_0 + (D_{s1} - D_{s2})\chi_p] = 0. \end{aligned} \tag{49}$$

Finally, undergo similar procession of amplitude and phase of in Eq. (49) as Eq. (31), and the stable–unstable regions are given in the (σ, χ) yield

$$\left(\sigma + \frac{C_N}{8\omega_m\beta_m}\chi_0^2\right)\left(\sigma + \frac{C_{s1} - C_{s2}}{8\omega_m\beta_m}\chi_0^2\right) = \frac{D_N^2\chi_0^4}{64\omega_m^2\beta_m^2}. \tag{50}$$

Based on definition of wavenumber, eigenfrequency and coefficient of mode coupling, we find that C_N, C_{s1}, C_{s2}, D_N, D_{s1}, D_{s2} are all functions of the radius of the tank, the liquid height, the gravitational intension and the sloshing damping. Hence, soft and hard spring characteristic and backbone curve will both vary over these parameters.

4.4. Numerical results and discussion

A circular cylindrical tank subjected to the pitch excitation is taken as a numerical example, where $a = 0.5\,\text{m}$, $h = 0.5\,\text{m}$, $e = 0.3\,\text{m}$, $\theta_0 = 0.1\,\text{rad}$.

The following conclusion can be made by the Fig. 2: corresponding to determinate liquid depth, the amplitude-frequency response exhibits a 'soft-spring' character in the planar motion and a 'hard-spring' in the rotary motion. A few cross-points of the left and right response curves of these two motions and stable–unstable boundary curves exist in the figure, three of which, $\sigma_1, \sigma_2, \sigma_3$, represent significant physical meanings that these three points are the boundary points of the physically realizable and unrealizable motions. And from Fig. 3, we can conclude that the system's amplitude-frequency response changes from a 'soft-spring' to a 'hard-spring' in the planar motion with the decreasing of the Bond number, while it changes from a 'hard-spring' to a 'soft-spring' in the rotary motion (critical value 10.224 ± 0.001). There are two reasons causing this change. One is derived from the gravity force and surface force's continuous trading-off in the sloshing, the other is derived from the liquid surface tension effect. Because of liquid viscous, liquid rises along tank wall, then more liquid adheres to tank wall in the coactions of surface tension and contact angle hysteresis. Liquid level rises, then sloshing mass falls, so sloshing character exhibits a significant change. Moreover,

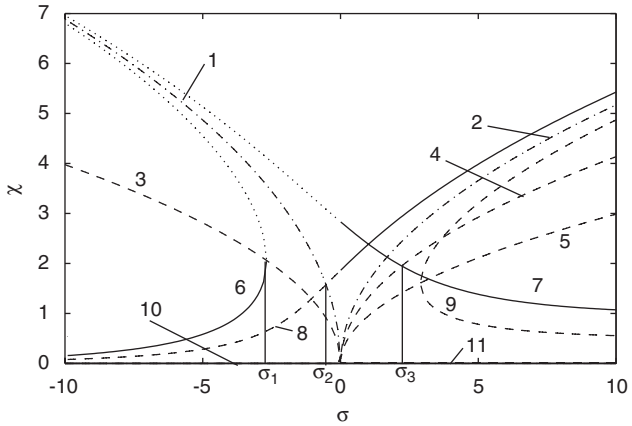

Fig. 2. Global response curves of the liquid sloshing in normal gravity under pitching excitation [6] (see Table 1 for explanation of curves and regions).

Table 1
Explanations for curves and regions in Figs. 2 and 3

Curve or region	Explanation	Equation
(1)	Backbone curve of planar motion	(30)
(2)	Backbone curve of rotary motion	(44)
(6), (7)	Response curve of planar motion	(30)
(8), (9)	Response curve of rotary motion	(44)
(3)–(1)	Unstable region for planar motion (jump phenomenon)	(37)
(1)–(4)	Unstable region for planar motion (appearance of rotary motion)	(50)
(2)–(5)	Unstable region for rotary motion (jump phenomenon)	(46)
(10)−(1), (4)−(11)	Unstable region for rotary motion (decay)	(50)

changing from a 'soft-spring' to a 'hard-spring' of the system's amplitude-frequency response will make the system presents different grade 'jump' and 'lag' phenomena.

Moreover, in the case of normal gravity condition, the response curves of planar motion and rotary motion and the unstable region are both clear. However, as the Bond number goes down, the distance between these curves will become smaller and smaller. That is to say, the difference between these motion types will become similarly smaller. So a small change of the exterior conditions may lead to a huge change of the system characteristic, even a mutation. This phenomenon can be represented by Fig. 3, in which as the exterior excitation changes, a jump from rotary motion to planar motion exists ($\sigma = \sigma_4$ and $\sigma = \sigma_5$). This is the jump phenomenon between different motion types. The stable region of the motion is illustrated in Fig. 4. And we can find that the stable region and type will demonstrate differently when the gravity condition varies. When Bond = 10 the stable region is not given in Fig. 4, because as the soft and hard characteristic changes, the original methods cannot be utilized to gain the stable region of the system, and other methods have to be used to solve this problem in future.

5. Conclusions

Under pitch excitation, the sloshing of liquid in circular cylindrical tank includes planar motion, rotary motion, rotary motion inside planar motion and other types. Planar motion may become unstable due to the jump phenomenon, or convert to rotary motion through out-of-surface motion. Similar phenomenon exits in the rotary motion. All these sloshing motions are connected to the radius of the tank, the liquid height, the

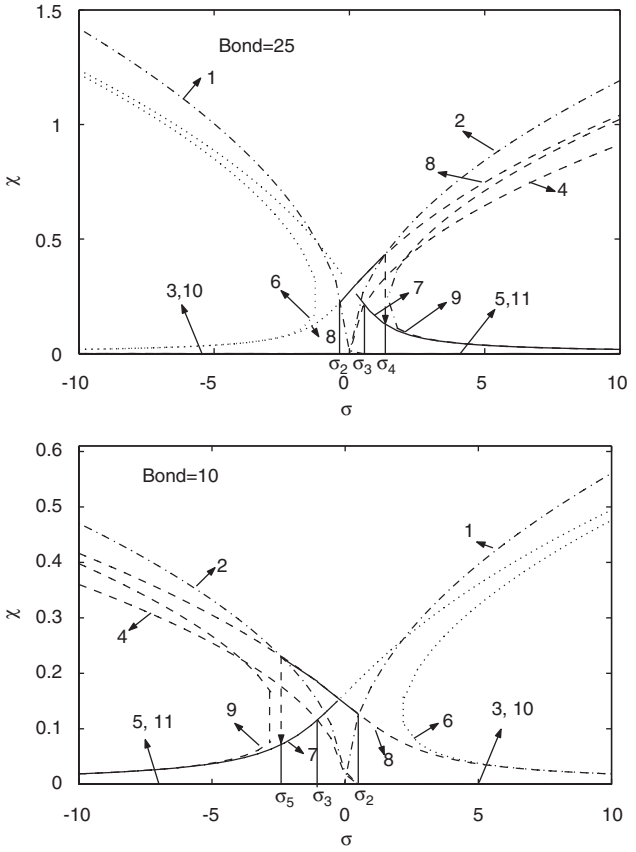

Fig. 3. Global response curves of the liquid sloshing in different Bond number under pitching excitation (see Table 1 for explanation of curves and regions).

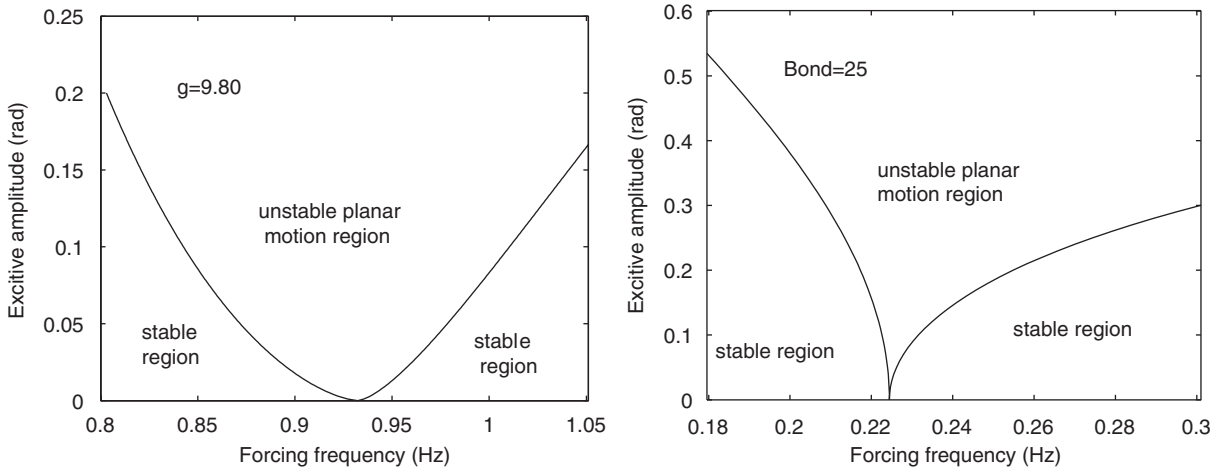

Fig. 4. The sketch of stable–unstable regions of the planar motion of liquid in different gravity under pitching excitation.

gravitational intension, surface tension and the sloshing damping. Hence, the soft and hard spring characteristic of backbone curve, grade bend, and stable–unstable region of these motions vary with the change of the parameter. The influence of the gravity condition on the liquid stable dynamics behaviors can be clearly illustrated by the response curves and all kinds of stable–unstable boundary in the (σ, χ) plane. The result indicates that the system's amplitude-frequency response changes from a 'soft-spring' to a 'hard-spring'

in the planar motion with the decreasing Bond number, while it changes from a 'hard-spring' to a 'soft-spring' in the rotary motion. Namely, the characteristic of the system will undergo a clear change in different gravity conditions and motion types.

Appendix

$$\lambda_i = k_i \tanh k_i h, \quad \tau = \int r\cos\theta[f(r)-C_0]\,\mathrm{d}s, \quad W^* = \int [f(r)-C_0]^2\,\mathrm{d}s, \quad \beta_i = \int \phi_i^2\,\mathrm{d}s,$$

$$\zeta_i = \int \phi_i z\cos\theta\,\mathrm{d}s\Big|_{r=a}, \quad \varsigma_i = \int \phi_i r\cos\theta\,\mathrm{d}s\Big|_{z=e-h}, \quad \delta_i = \int \phi_i \Phi_0\,\mathrm{d}s, \quad \tau_i = \int r\cos\theta\phi_i\,\mathrm{d}s,$$

$$\psi_i = \frac{\partial\phi_i}{\partial r}, \quad \chi_i = \frac{1}{r}\frac{\partial\phi_i}{\partial\theta}, \quad W_i = \int \psi_i\cdot z\cos\theta[f(r)-C_0]\,\mathrm{d}s,$$

$$V_i = \int \chi_i\cdot\frac{z\sin\theta}{r}[f(r)-C_0]\,\mathrm{d}s, \quad U_i = \int \phi_i\cdot r\cos\theta[f(r)-C_0]\,\mathrm{d}s,$$

$$P_i = \int \phi_i[f(r)-C_0]\,\mathrm{d}s, \quad Q_i = \int \psi_i\cos\theta[f(r)-C_0]^2\,\mathrm{d}s,$$

$$\mathrm{I}Q_i = \int \psi_i\cdot z\cos\theta[f(r)-C_0]^2\,\mathrm{d}s, \quad O_i = \int \chi_i\cdot\sin\theta[f(r)-C_0]^2\,\mathrm{d}s,$$

$$\mathrm{I}O_i = \int \chi_i\cdot z\sin\theta[f(r)-C_0]^2\,\mathrm{d}s, \quad \mathrm{I}P_i = \int \phi_i\cdot r\cos\theta[f(r)-C_0]^2\,\mathrm{d}s,$$

$$X_{ij} = \int \phi_i\phi_j[f(r)-C_0]\,\mathrm{d}s, \quad P_{ij} = \int \psi_i\psi_j[f(r)-C_0]\,\mathrm{d}s,$$

$$O_{ij} = \int \chi_i\chi_j[f(r)-C_0]\,\mathrm{d}s, \quad \mathrm{I}W_{ij} = \int \psi_i\phi_j\cdot\cos\theta[f(r)-C_0]\,\mathrm{d}s,$$

$$\mathrm{I}V_{ij} = \int \psi_i\phi_j\cdot z\cos\theta[f(r)-C_0]\,\mathrm{d}s, \quad \mathrm{I}U_{ij} = \int \chi_i\phi_j\cdot z\sin\theta[f(r)-C_0]\,\mathrm{d}s,$$

$$\mathrm{I}P_{ij} = \int \chi_i\phi_j\cdot\sin\theta[f(r)-C_0]\,\mathrm{d}s, \quad \mathrm{I}O_{ij} = \int \phi_i\phi_j\cdot r\cos\theta[f(r)-C_0]\,\mathrm{d}s,$$

$$\mathrm{I}R_{ij} = \int \psi_i\psi_j[f(r)-C_0]^2\,\mathrm{d}s, \quad \mathrm{I}S_{ij} = \int \chi_i\chi_j[f(r)-C_0]^2\,\mathrm{d}s,$$

$$E^*_{ij} = \int \psi_i\phi_j\cdot z\cos\theta\,\mathrm{d}s, \quad F^*_{ij} = \int \chi_i\phi_j\cdot z\sin\theta\,\mathrm{d}s, \quad G^*_{ij} = \int \phi_i\phi_j\cdot r\cos\theta\,\mathrm{d}s,$$

$$Y^*_{ij} = \int \phi_i\phi_j[f(r)-C_0]^2\,\mathrm{d}s,$$

$$\beta^k_{ij} = \int \psi_i\psi_j\phi_k\,\mathrm{d}s, \quad \gamma^k_{ij} = \int \chi_i\chi_j\phi_k\,\mathrm{d}s, \quad \alpha^k_{ij} = \int \phi_i\phi_j\phi_k\,\mathrm{d}s,$$

$$H^*_{ijk} = \int \psi_i\phi_j\phi_k\cdot\cos\theta\,\mathrm{d}s, \quad I^*_{ijk} = \int \psi_i\phi_j\phi_k\cdot z\cos\theta\,\mathrm{d}s,$$

$$J^*_{ijk} = \int \chi_i\phi_j\phi_k\cdot\sin\theta\,\mathrm{d}s, \quad K^*_{ijk} = \int \chi_i\phi_j\phi_k\cdot z\sin\theta\,\mathrm{d}s,$$

$$L^*_{ijk} = \int \phi_i\phi_j\phi_k\cdot r\cos\theta\,\mathrm{d}s, \quad \mathrm{I}T_{ijk} = \int \phi_i\phi_j\phi_k[f(r)-C_0]\,\mathrm{d}s,$$

$$R_{ijk} = \int \psi_i\psi_j\phi_k[f(r)-C_0]\,\mathrm{d}s, \quad S_{ijk} = \int \chi_i\chi_j\phi_k[f(r)-C_0]\,\mathrm{d}s,$$

$$\Gamma^{kl}_{ij} = \int \phi_i\phi_j\phi_k\phi_l\,\mathrm{d}s, \quad \Lambda^{kl}_{ij} = \int \psi_i\psi_j\phi_k\phi_l\,\mathrm{d}s, \quad \Delta^{kl}_{ij} = \int \chi_i\chi_j\phi_k\phi_l\,\mathrm{d}s, \quad \Pi^{kl}_{ij} = k_j^2\Gamma^{kl}_{ij} + \Lambda^{kl}_{ij} + \Delta^{kl}_{ij}.$$

References

[1] A.R. Ibrahim, *Liquid Sloshing Dynamics*: *Theory and Applications*, Cambridge University Press, Cambridge, 2005, pp. 1–20.
[2] X. Ma, B. Wang, X. Gou, *Research and Application of Some Problems in the Spacecraft Dynamics*, Science Press, 2001, pp. 1–29 (in Chinese).
[3] R.E. Hutton, An investigation of resonant, nonlinear, nonplanar free surface oscillations of a fluid, *NASA TN D-1870*, 1963.
[4] X. Gou, X. Ma, B. Wang, T. Li, H. Huang, Synchronous Hopf bifurcation and damping osmosis phenomena of a liquid-spacecraft nonlinear coupling system, *AIAA Journal* 39 (2) (2001) 225–232.
[5] K. Komatsu, Nonlinear sloshing analysis of liquid in tanks with arbitrary geometries, *International Journal of Nonlinear Mechanics* 22 (3) (1987) 193–207.
[6] L. Yin, B. Wang, X. Ma, J. Zou, The nonlinear sloshing of liquid in tank with pitching, *Transactions of ASME, Journal of Applied Mechanics* 66 (4) (1999) 1032–1034.
[7] M. Utsumi, Low-gravity propellant slosh analysis using spherical coordinates, *Journal of Fluids and Structures* 12 (1998) 57–83.
[8] M. Utsumi, Development of mechanical models for propellant sloshing in teardrop tanks, *Journal of Spacecraft and Rockets* 37 (5) (2000) 597–603.
[9] H.A. Snyder, Sloshing in microgravity, *Cryogenics* 39 (1999) 1047–1055.
[10] L.D. Peterson, E.F. Crawley, R.J. Hansman, The nonlinear dynamics of a spacecraft coupled to the vibration of a contained fluid, *AIAA Paper 88–2470*, 1988.
[11] M.C. Van Schoor, E.F. Crawley, Nonlinear forced-response characteristics of contained fluids in microgravity, *Journal of Spacecraft and Rockets* 32 (3) (1995) 521–532.
[12] D.D. Waterhouse, Resonant sloshing near a critical depth, *Journal of Fluid Mechanics* 281 (1994) 313–318.
[13] J.C. Luke, A variational principle for a fluid with a free surface, *Journal of Fluid Mechanics* 27 (2) (1967) 395–397.